EUROPEAN ORGANIZATION FOR NUCLEAR RESEARCH

L3 Note 2560
June 28, 2000

Search for Colour Reconnection Effects in $e^+e^- \to W^+W^- \to$ hadrons

The L3 Collaboration

Abstract

We report on preliminary studies of colour reconnection effects in hadronic decays of W pairs with the L3 detector. The analysis is based on a comparison of charged particle multiplicities in $qqqq$ and $qq\ell\nu$ events at centre-of-mass energies between 183 and 202 GeV, and on the study of the particle and energy flow between jets associated to the same W boson and between two different W bosons in $qqqq$ events at 189 GeV centre-of-mass energy.
The interjet activity shows sensitivity to hadronisation models incorporating various colour reconnection schemes. A quantitative comparison between our 189 GeV data and Monte Carlo samples with and without colour reconnection is made.

Submitted to the *XXXth International Conference on High Energy Physics*
July 27 - August 2, 2000, Osaka, Japan

1 Introduction

In the process e$^+$e$^-$ $\rightarrow$ W$^+$W$^-$ $\rightarrow$ hadrons it has been suggested that interactions may occur between the decay products of the two W bosons [1–4]. As a result the colour flow pattern of these events are modified. Colour rearrangement between two colour singlets are expected from simple QCD principles.

The W bosons produced in e^+e^- annihilation decay at short distances ($\approx$ 0.1 fm). Consequently, the hadronisation of the two quark pairs occurs with a large space-time overlap, since the typical hadronic scale is about 1 fm. Colour reconnection (CR) effects are thought to be suppressed in the hard perturbative phase, but may have larger effects in the non-perturbative stage of the hadronisation process [2]. While hard gluons ($E_g > \Gamma_W$) are emitted incoherently by the two original colour singlets only soft gluons could in principle feel the collective action of both systems and thus participate in cross-talks. The net effect should appear in inclusive soft particle distributions as a change of the mean particle multiplicity as well as a change in momentum spectra.

In the absence of any cross-talk one can imagine 2 strings being stretched between the two quarks from the two W bosons as shown in Figure 1a). Subsequently these 2 strings fragment to produce the hadrons which can be uniquely assigned to a W boson. In case of colour

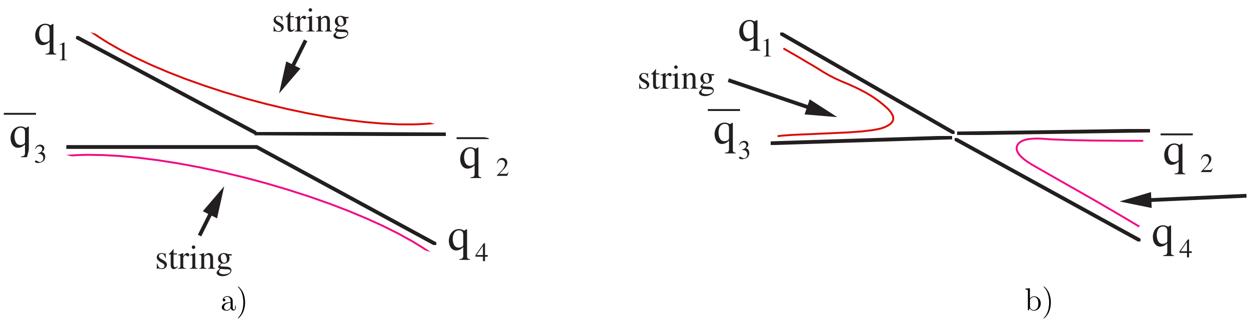

Figure 1: Coloured string topology in W$^+$W$^-$ $\rightarrow q_1\bar{q}_2\bar{q}_3q_4$ for a) no cross talk and b) immediate reconnection scenario.

reconnection the modifications of this simple string topology picture would result in some depletion and/or enhancement of soft particles in particular phase space regions, especially between the jets. Figure 1b) shows an other topology where the strings are stretched between quarks of different W bosons. It corresponds to the immediate reconnection scenario [1] which is very unlikely to happen but gives the strongest effect on the interjet particle activity.

In this note we report on an experimental study of colour reconnection effects in WW events selected by L3. In Section 2 we study the inclusive charged particle multiplicity and multiplicities as a function of particle momentum in $qqqq$ and $qq\ell\nu$ events, in data taken at centre-of-mass energies between 183 and 202 GeV. Section 3 describes the analysis using the new method [5] based on the study of the energy flow and particle flow distributions in 4-jet events to search for effects of particle depletion and enhancement in a model independent way, using data taken at $\sqrt{s}$ = 189 GeV. The analysis presented here is an update of the analysis presented in Reference 6. The L3 detector is described in detail in Reference 7. All results are preliminary.

2 Charged Particle Multiplicities

It is interesting to study the possible difference between the average charged particle multiplicity in $qqqq$ events, and twice the average charged particle multiplicity in $qq\ell\nu$ events, of course with the lepton tracks subtracted. Since there can be no colour reconnection in $qq\ell\nu$ events, these events serve as a good reference sample; the comparison of data with data allows a study of colour reconnection with reduced systematic errors. Many colour reconnection models predict a decrease of charged particle multiplicity in $qqqq$ events, especially at low momentum. It should be noted that also some models of Bose-Einstein correlations predict a change in multiplicity, typically increasing the multiplicity in $qqqq$ events [8].

Table 1 shows $\sqrt{s}$ and the integrated luminosity of the samples used in this study. Runs failing certain criteria on the data quality of the central tracking chamber TEC are excluded from the analysis.

The selection of the WW event samples used in the multiplicity analysis is described in References 9 and 10. The number of selected $qqqq$ and $qq\ell\nu$ events is given in Table 1. In total, 3753 $qqqq$ events, and 2642 $qq\ell\nu$ events are selected in 452.6 pb^{-1} of high energy data.

The background is dominated by $q\bar{q}(\gamma)$ events and ZZ events, and has a small contribution from Zee events; these processes are modeled with PYTHIA [11] and, for $q\bar{q}(\gamma)$, KK2F [12]. All Monte Carlo events are processed through a realistic L3 detector simulation.

The charged particle multiplicity in the hadronic final state of $qq\ell\nu$ and $qqqq$ events is studied by selecting tracks reconstructed in the central tracking chamber TEC, and correcting for selection and acceptance effects, detector inefficiencies, and ISR.

Tracks are accepted if they have a fitted transverse momentum of more than 100 MeV, a radial distance of closest approach to the interaction point of less than 10 mm, at least 25 out of 62 possible hits on the track, and a ratio of number of hits on the track over the track span of more than 0.5. The cut on the number of hits implies that the track must be within $|\cos\theta| < 0.88$, where θ is the polar angle of the track with respect to the beam axis. The observed track multiplicities are corrected for the background, using the track multiplicities predicted by the background Monte Carlo. In $qq\ell\nu$ events, the lepton track(s) is (c.q. are) subtracted in order to study only the hadronic final state. Events without any accepted tracks are rejected.

Figure 2 shows the observed track multiplicity distribution for $qqqq$ and $qq\ell\nu$ events in the 189 GeV data, compared to the Monte Carlo predictions. The track multiplicity distribution is transformed into a charged particle multiplicity distribution by unfolding it with a matrix $P(N_p, N_t)$, obtained from fully simulated KORALW Monte Carlo events, representing

$\sqrt{s}$ [GeV]	$\mathcal{L}$ [pb^{-1}]	N_{qqqq}	$N_{qq\ell\nu}$
182.7	55.5	467	297
188.6	176.4	1512	1033
191.6	29.0	225	183
195.5	82.4	633	513
199.5	72.5	620	404
201.8	36.8	296	212

Table 1: Centre-of-mass energies $\sqrt{s}$, integrated luminosities $\mathcal{L}$, number of selected $qqqq$ events N_{qqqq}, and number of selected $qq\ell\nu$ events $N_{qq\ell\nu}$ in the L3 data from 1997 to 1999.

Source	N_{qqqq}	$N_{qq\ell\nu}$	ΔN
track selection	0.38	0.21	0.21
event selection	0.12	0.11	0.14
unfolding procedure	0.03	0.03	0.04
background	0.16	0.08	0.14
fragmentation	0.20	0.12	0.20
CR models	0.18	-	0.18
total	0.51	0.28	0.40

Table 2: Systematic errors on the $qqqq$ and $qq\ell\nu$ average hadronic multiplicities, and on the difference ΔN, at $\sqrt{s} = 189$ GeV.

the probability to select N_t tracks when N_p charged particles were generated. Charged particles are considered stable when they have a lifetime of more than $3.3 \cdot 10^{-10}$ s, whereas particles with shorter lifetime are allowed to decay.[1)] The multiplicity distribution is then corrected for the effects of ISR.

Alternatively, the distribution of the variable $\xi_p = -\log(x_p)$ is made, where $x_p = 2p/\sqrt{s}$ is the scaled momentum of each track. This distribution is corrected bin-by-bin for acceptance and selection effects and ISR using KORALW. The average charged particle multiplicity as a function of ξ_p is shown in Figure 3 (top) for 189 GeV data and Monte Carlo. In the comparison with $qqqq$ events, histograms containing $qq\ell\nu$ events are scaled up by a factor 2. The same plots for the data at 192-202 GeV are shown in Figure 4. By integrating the ξ_p distribution, the average charged particle multiplicity is determined. In Figure 3 (bottom), the $qq\ell\nu$ ξ_p distribution is subtracted from the $qqqq$ ξ_p distribution, in 189 GeV data as well as in Monte Carlo. The same is done in Figure 4 for the 192-202 GeV data.

Systematic uncertainties arising from track selection and Monte Carlo simulation of the track reconstruction are studied with a reference sample consisting of hadronic ($\mathrm{q\bar{q}}(\gamma)$) events selected from the 189 GeV data. The influence of event selection is studied by varying the selection criteria. Track selection effects are estimated by selection cut variation. The normalisation of the background is varied. Systematics arising from the correction procedure are studied by performing the correction with the various Monte Carlo programs used in this analysis, with and without colour reconnection. The systematic errors in the 189 GeV data are given in Table 2. Systematic errors in the 192-202 GeV data are similar.

A final result on the average charged particle multiplicity is obtained from the two methods described above, taking their (small) difference as an additional systematic error. The results are given in Table 3.

Combining all data, taking into account their correlations, and assuming the multiplicity to be independent of $\sqrt{s}$, we obtain:

$$< N_{ch}^{qqqq} > \; = \; 37.90 \pm 0.14 \pm 0.41 \qquad (1)$$

$$< N_{ch}^{qq\ell\nu} > \; = \; 19.09 \pm 0.11 \pm 0.21\,, \qquad (2)$$

where the first error is statistical and the second systematic. Our KORALW+JETSET Monte

[1)] In our earlier analyses of the hadronic multiplicities in WW events, K^0_S's, Λ's, etc. that traversed the TEC before decaying were not properly taken into account in this definition. This leads to a correction of +1.3% for the $qqqq$ and $qq\ell\nu$ multiplicities, in data and MC, at 183 and 189 GeV; the difference between the two is however not affected, and neither are the conclusions of the previous analyses.

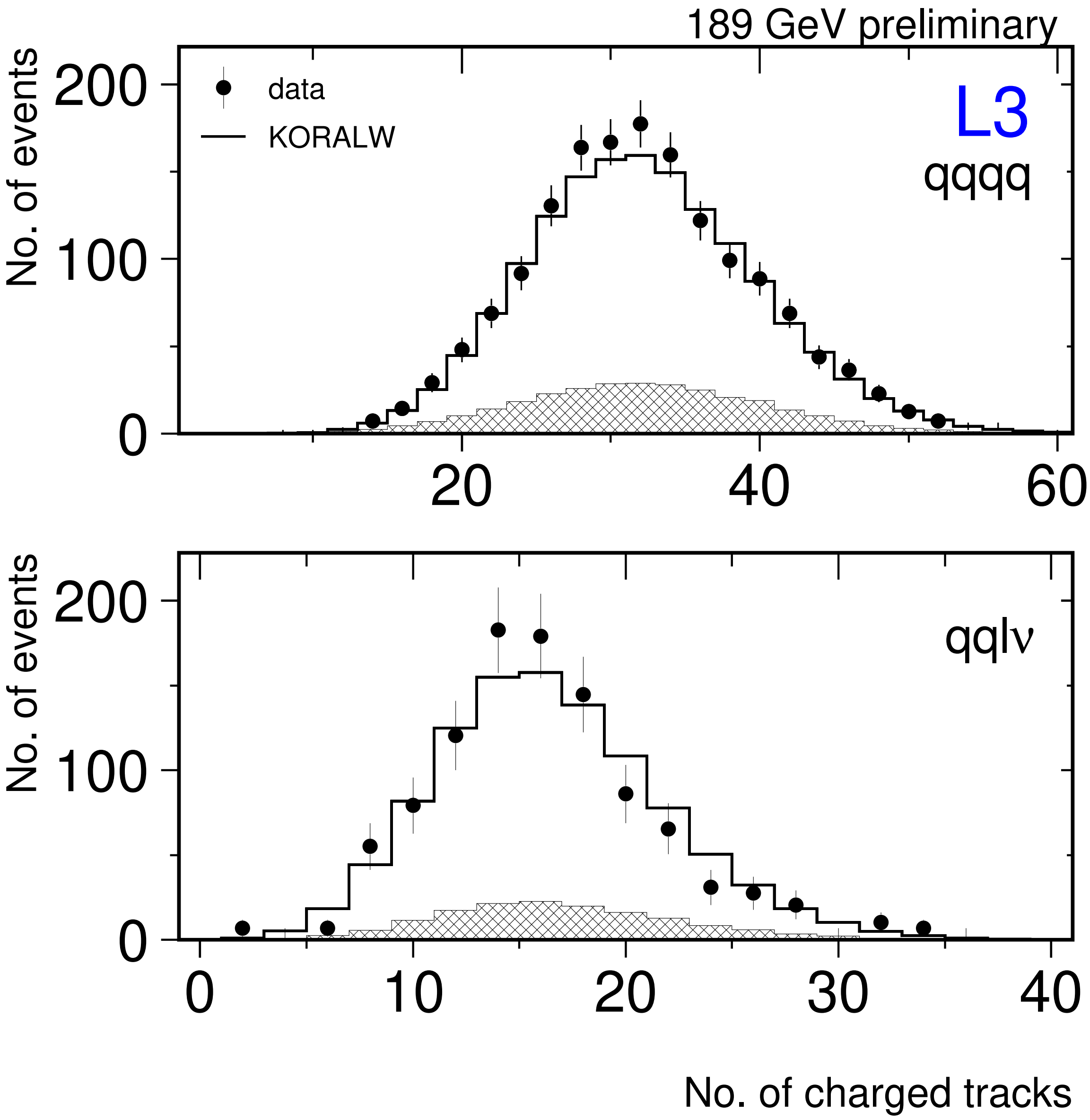

Figure 2: Uncorrected charged track multiplicity in $qqqq$ data (top) and $qq\ell\nu$ data (bottom), compared to the KORALW predictions, at $\sqrt{s} = 189$ GeV. The hatched histogram represents the background, which is dominated by $q\bar{q}(\gamma)$ with a smaller component from ZZ and Zee.

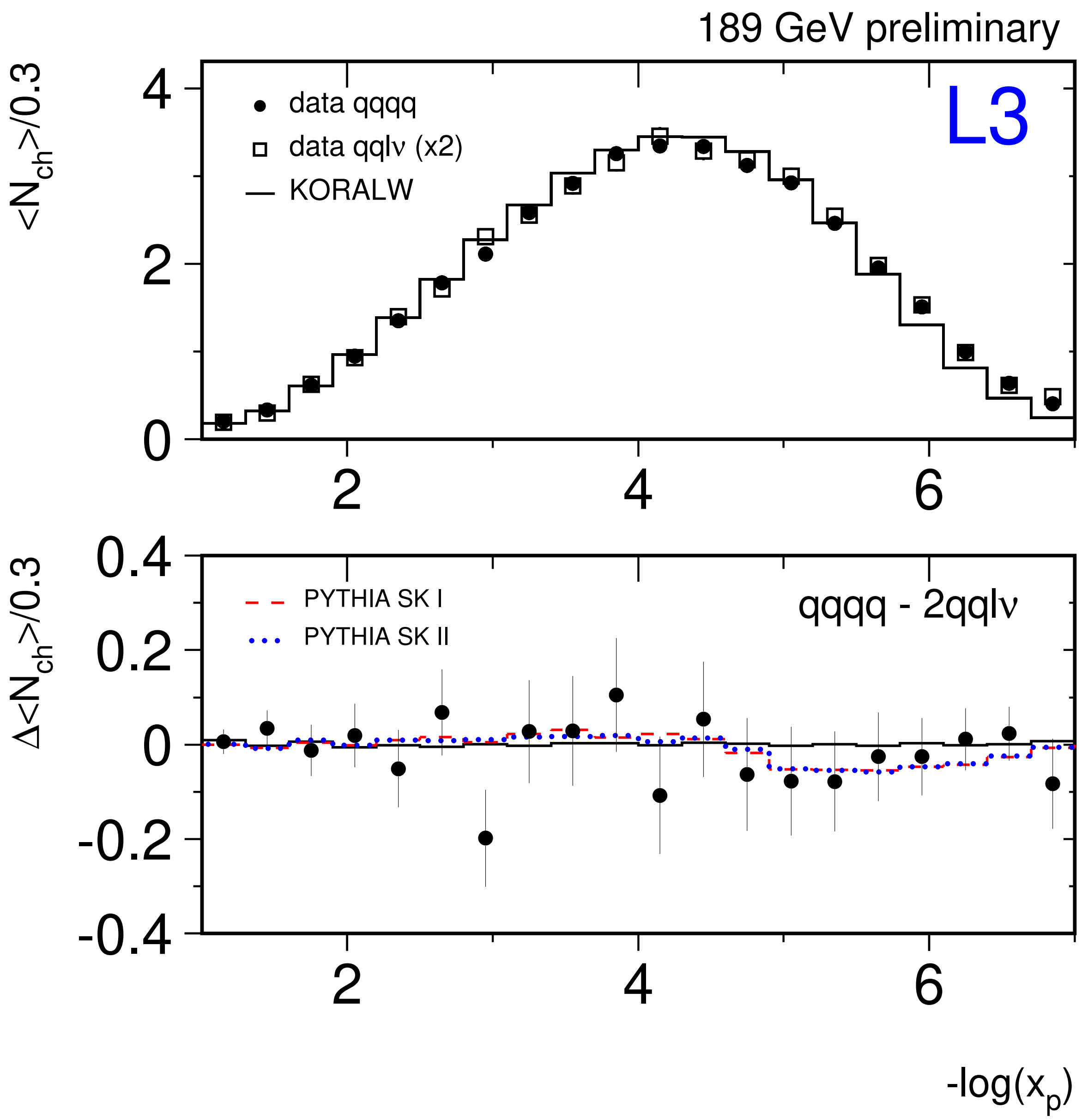

Figure 3: Top: Average charged particle multiplicity as a function of $\xi_p = -\log(x_p)$, where x_p is the scaled particle momentum, for $qqqq$ and $qq\ell\nu$ data at 189 GeV, and according to the prediction of KORALW. Bottom: Difference in average charged particle multiplicity between $qqqq$ and $qq\ell\nu$ data as a function of $-\log(x_p)$, and idem for Monte Carlo. In these histograms, the $qq\ell\nu$ data and MC are scaled up by a factor of 2.

$\sqrt{s}$ [GeV]	$< N_{ch}^{qqqq} >$	$< N_{ch}^{qq\ell\nu} >$	$\Delta < N_{ch} >$
182.7	$37.22 \pm 0.41 \pm 0.78$	$18.81 \pm 0.30 \pm 0.42$	$-0.40 \pm 0.72 \pm 0.56$
188.6	$37.66 \pm 0.22 \pm 0.51$	$18.95 \pm 0.17 \pm 0.28$	$-0.23 \pm 0.40 \pm 0.40$
191.6	$38.91 \pm 0.60 \pm 0.56$	$19.31 \pm 0.43 \pm 0.33$	$+0.30 \pm 1.05 \pm 0.45$
195.5	$37.82 \pm 0.35 \pm 0.55$	$19.12 \pm 0.26 \pm 0.33$	$-0.42 \pm 0.63 \pm 0.45$
199.5	$37.85 \pm 0.36 \pm 0.55$	$19.49 \pm 0.30 \pm 0.33$	$-1.14 \pm 0.70 \pm 0.45$
201.8	$38.34 \pm 0.52 \pm 0.56$	$19.09 \pm 0.40 \pm 0.32$	$+0.16 \pm 0.95 \pm 0.45$

Table 3: Centre-of-mass energies $\sqrt{s}$, average charged hadronic multiplicity in $qqqq$ events $< N_{ch}^{qqqq} >$, average charged hadronic multiplicity in $qq\ell\nu$ events $< N_{ch}^{qq\ell\nu} >$, and the difference $\Delta < N_{ch} >=< N_{ch}^{qqqq} > -2 < N_{ch}^{qq\ell\nu} >$ in the L3 data from 1997 to 1999.

Carlo, with our tuning, predicts for these numbers 37.64 and 18.82 respectively. A common LEP sample of KORALW+JETSET events with tuning according to the ALEPH experiment [2)] predicts 37.96 and 18.98; a similar sample of KORALW+HERWIG events predicts 38.03 and 19.01. The same KORALW+JETSET events, but 100% colour-reconnected following the SK I algorithm with $k \to \infty$, have a multiplicity of 37.43 for the $qqqq$ events. The statistical error for these Monte Carlo predictions is approximately 0.03 per sample.

The difference between the average charged particle multiplicity in $qqqq$ and $qq\ell\nu$ events is thus determined to be:

$$\Delta < N_{ch} > \; = \; -0.29 \pm 0.26 \pm 0.30\,, \qquad (3)$$

where $\Delta < N_{ch} >=< N_{ch}^{qqqq} > -2 < N_{ch}^{qq\ell\nu} >$. This result is statistically consistent with 0, as well as with the SK colour reconnection model predictions (for SK I -0.1 to -0.2 for $k = 0.6$ and -0.5 for $k \to \infty$), and cannot discriminate between them.

The dispersions D of the corrected charged multiplicity distributions for $qqqq$ and $qq\ell\nu$ events in the 189 GeV data are calculated over the full width of the distributions and are found to be:

$$D^{qqqq} = 8.12 \pm 0.17 \pm 0.43 \qquad (4)$$
$$D^{qq\ell\nu} = 5.97 \pm 0.14 \pm 0.38\,, \qquad (5)$$

leading to a difference $\Delta D = D^{qqqq} - \sqrt{2} D^{qq\ell\nu} = -0.32 \pm 0.33 \pm 0.29$, with KORALW predicting $\Delta D = -0.02 \pm 0.03$.

3 Inter-Jet Particle- and Energy Flow

3.1 Data sample and event selection

The selection of $e^+e^- \to W^+W^- \to$ hadrons events used in the particle- and energy flow analysis is based on the energy measured in the electromagnetic and hadronic calorimeters and in the tracking chamber. We measure the total visible energy ($E_{\rm vis}$) and the energy imbalance parallel ($E_{\parallel}$) and perpendicular ($E_{\perp}$) to the beam direction. The number of clusters, defined as

[2)] These MC event samples are known within the LEP experiments as the "Crete" event samples, and have been generated as part of a set for common systematic studies among the LEP experiments.

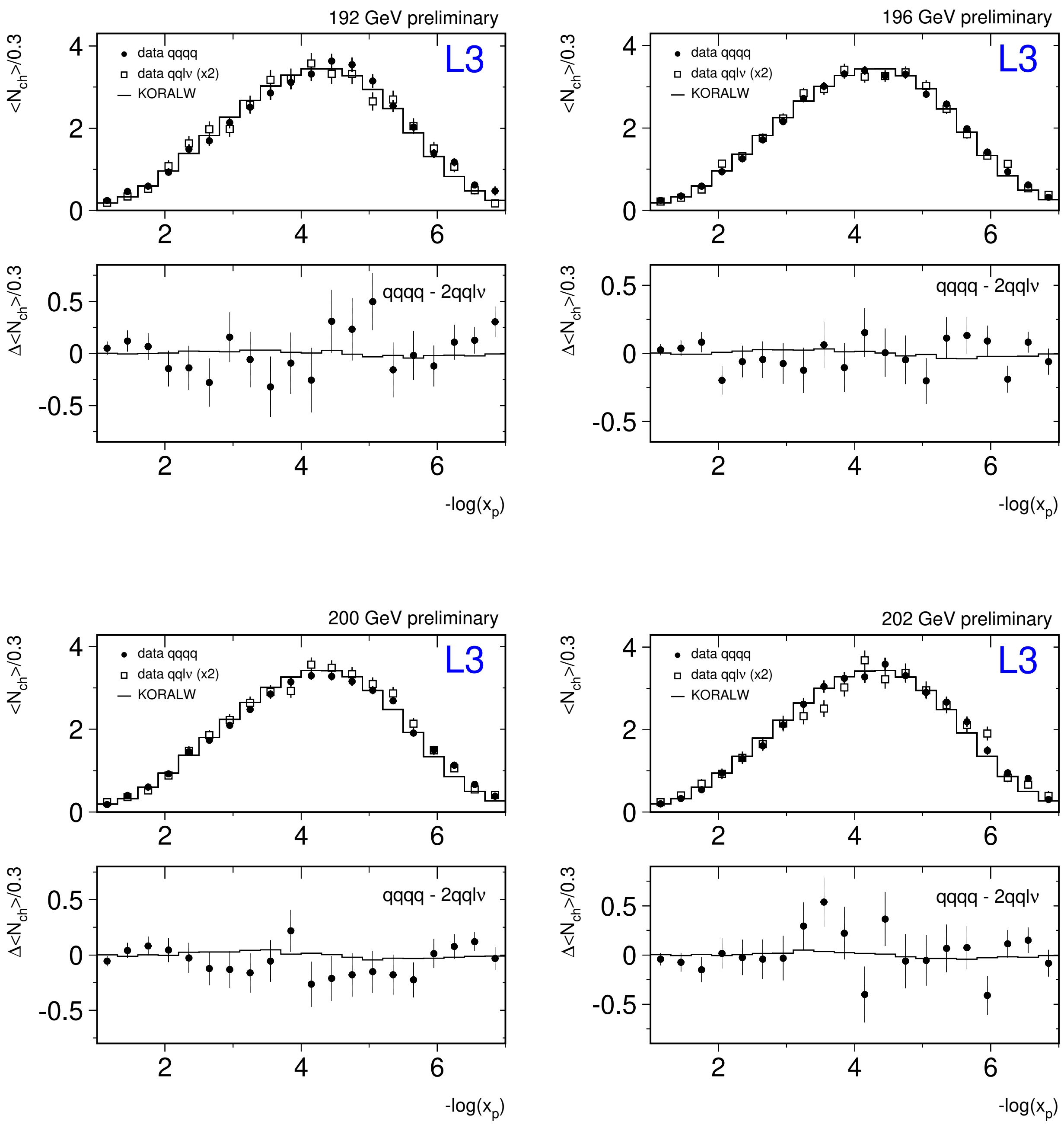

Figure 4: As Figure 3 for the data at 192-202 GeV.

objects obtained from a non-linear combination of energies of charged tracks and calorimetric clusters with a minimum energy of 100 MeV, is denoted by N_{cluster}. The selection criteria are:

- $E_{\text{vis}}/\sqrt{s} > 0.7$; $E_{\perp}/E_{\text{vis}} < 0.2$; $|E_{\parallel}|/E_{\text{vis}} < 0.2$; $N_{\text{cluster}} \geq 40$.

In addition the events should have 4 jets reconstructed with the Durham algorithm with $y_{cut} = 0.01$. To reduce the contamination from hard initial state radiation (ISR) and from semileptonic W decays, we apply cuts to reject events with energetic $\gamma, \mu^{\pm}$ and $e^{\pm}$.

For the study of the particle- and energy flow between jets, the initial quark configuration should be well reconstructed with a nearly perfect quark-jet association. At 189 GeV, the W bosons produced in e^+e^- annihilation have a non negligible boost and this property is used to select unambiguous topologies in a sample of 4-jet events. This selection is made in such a way as to select topologies corresponding to Figure 1a), and to prevent the selection of events where the two strings cross each other and for which the cross-talk effects cannot be easily traced.

The criteria correspond to cuts on the four interjet angles. The two largest interjet angles should be between 100° and 140° and not adjacent. The two other interjet angles should be less than 100°. This selection guarantees similar sharing of energy between the four primary partons with the two string evolving back to back. These cuts have been chosen by studying Monte Carlo $\mathrm{W^+W^-}$ events.

Applying all the cuts the final sample at 189 GeV contains 209 events with an efficiency of 15% and a purity of 85% for $\mathrm{e^+e^-} \rightarrow \mathrm{W^+W^-} \rightarrow \mathrm{q\,\bar{q}q\,\bar{q}}$. The background is composed of $q\bar{q}(\gamma)$ events, and ZZ events in similar amounts. For this study the $q\bar{q}(\gamma)$ process has been modeled with KK2F Monte Carlo program [12]. The probability to have the right pairing (i.e. the topology of Figure 1) is estimated to be 87%.

The normalised visible energy and the thrust distributions after selection are shown in Figure 5 for data and Monte Carlo predictions. The distributions of the four interjet angles are shown in Figure 6. The agreement between data and Monte Carlo is satisfactory.

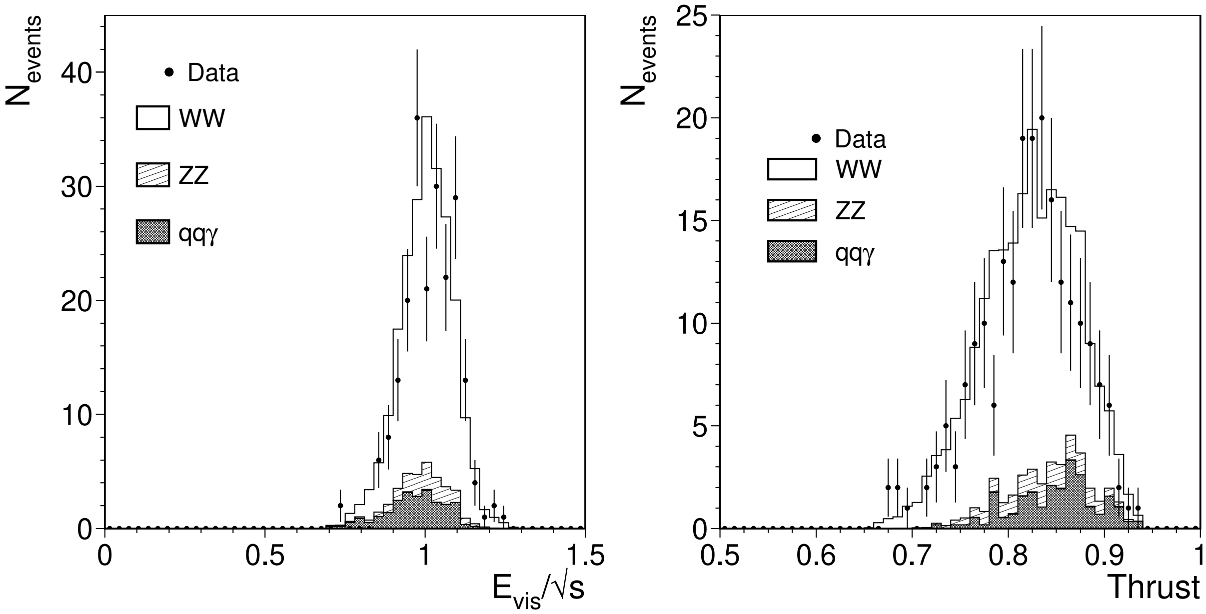

Figure 5: Normalised visible energy and thrust distributions for selected events.

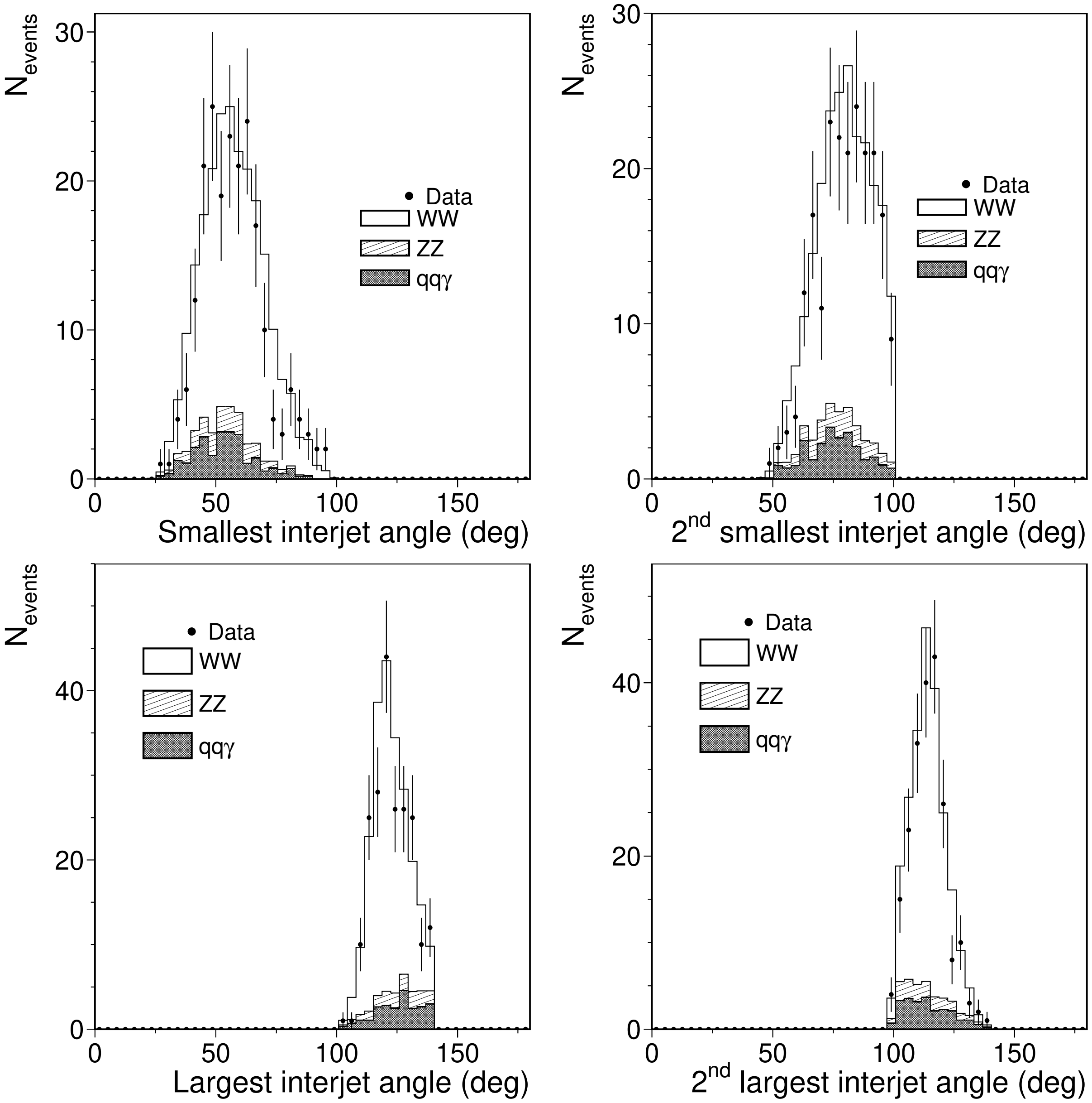

Figure 6: Distributions of the 4 interjet angles after selection.

3.2 Flow distributions

We start by defining the plane spanned by the most energetic jet (jet 1) and the jet associated to the same W (jet 2) (Figure 7). For each event we project the direction of all the particles onto this plane. The energy and particle flows are measured as a function of the angle on the plane between the jet 1 and the projected momentum vector. This angle is defined as increasing from jet 1 toward jet 2 (from same W), then to the closest jet from the other W (jet 3) toward the remaining jet (jet 4) and back to jet 1. A particle i making an angle ϕ_i with respect to jet 1 adds an entry equal to 1 in the particle flow and adds an entry equal to its energy in the energy flow for the corresponding ϕ bin.

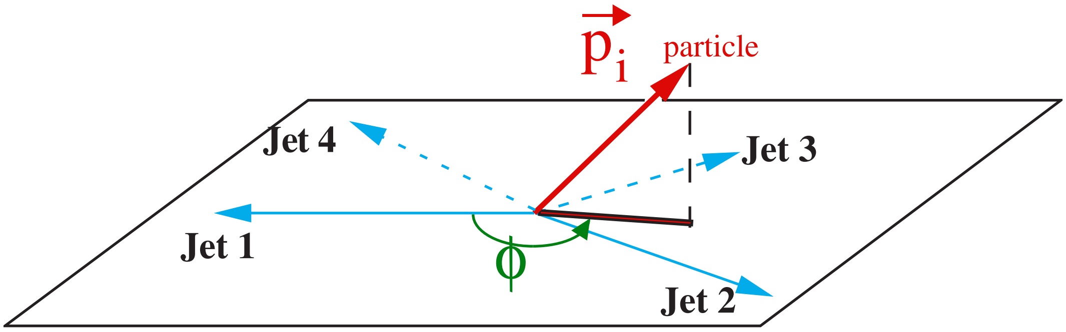

Figure 7: Illustration of the method used to build the flow distributions

The distributions are calculated for three different particle definitions:

- The clusters built from tracking and calorimetric information of more than 100 MeV
- The tracks with momentum $p > 100$ MeV
- The tracks with momentum p such that 0.1 GeV $< p < 1$ GeV

The particle flow distribution obtained with clusters is shown in Figure 8(left) for the data and the Monte Carlo predictions. Before the background subtraction no normalisation is attempted for particle flow.

Figure 8(right) shows the energy flow obtained with the clusters. The contribution of each event to the energy flow is normalised to the total event energy.

The 4-jet structure is clearly visible with the decay products of one W covering the region starting from 0 to ≈ 120 degrees while the second W covers the angular region from 140 to 340 degrees.

Having one jet as a reference for all particles makes the direct comparison of the jet1-jet2 particle activity with the jet3-jet4 particle activity difficult. In order to compare the interjet regions the angles on the plane are redefined using a rescaling procedure making use of the relative angle of the particle with the two closest jets. For a particle i located between jets j and k the rescaled angle is: $\phi_i^{\mathrm{resc}} = \phi_i/\phi_{jk}$ where ϕ_{jk} is the angle between jets j and k. With this definition the four jets have fixed rescaled angle values equal to 0, 1, 2 and 3.

A second transformation is performed in order to take into account the fact that the W events are not planar. Figure 9 shows the angle α between the two W decay planes defined by the (jet1-jet2) plane and the (jet3-jet4) plane.

This transformation consists of using four planes for projecting the particles instead of only one. The four planes correspond to the planes spanned by each pair of adjacent jets. The

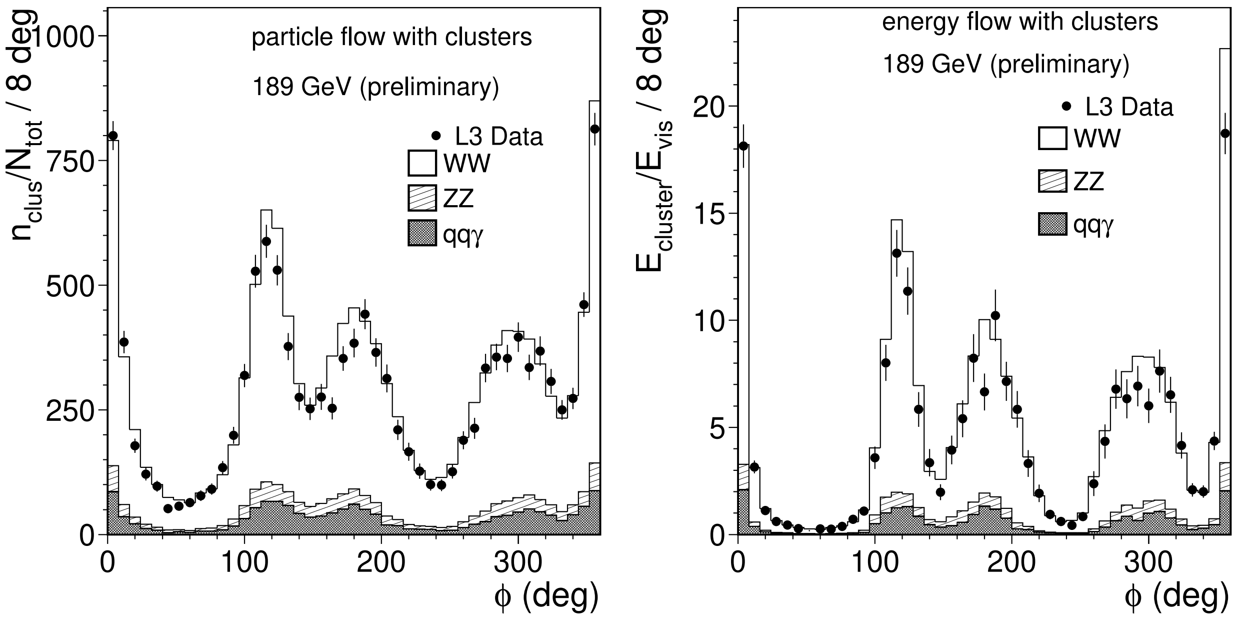

Figure 8: Particle and energy flow distributions obtained with clusters at $\sqrt{s}$ = 189 GeV for data and Monte Carlo predictions.

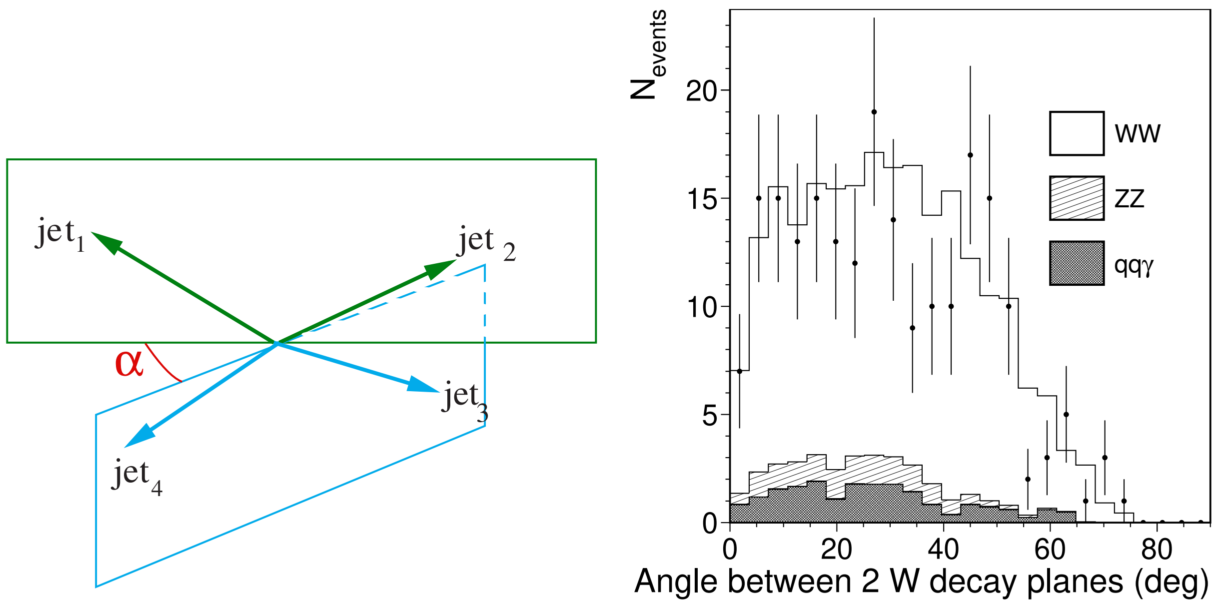

Figure 9: Distribution of the angle between the 2 reconstructed W decay planes at $\sqrt{s}$ = 189 GeV.

particles located between two jets are then projected only on the plane spanned by these two jets. Thus the colour pattern existing between the two partons can be studied.

Figure 10 (left) shows the rescaled normalised particle flow obtained with clusters after background subtraction. The line corresponds to the standard KORALW prediction for $q\bar{q}q\bar{q}$ events without CR. The distribution obtained with tracks of momentum less than 1 GeV is shown in Figure 10 (right). It should be noticed that the choice of four planes helps in symmetrising the flow distributions: the interjet activity in the regions corresponding to the two W "strings" in the Monte Carlo are now identical as expected. (This was not the case before this procedure). In the presence of cross-talk between W's such a symmetry may be broken.

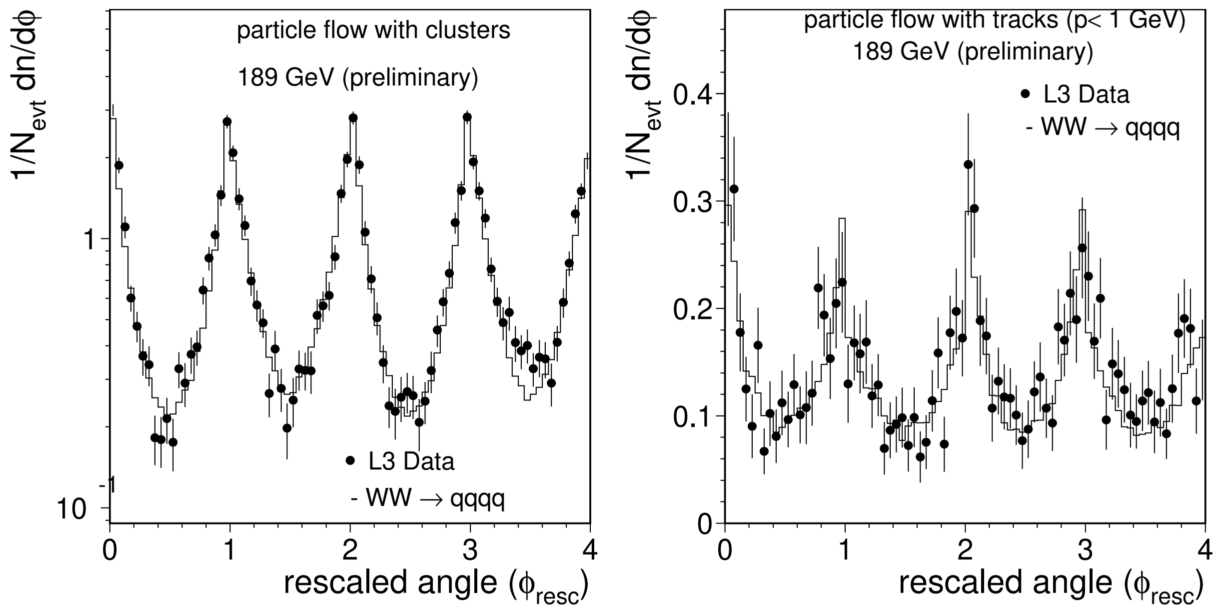

Figure 10: Particle flow distributions as a function of the rescaled angle for data and KORALW prediction at $\sqrt{s} = 189$ GeV.

3.3 Model predictions

The study is performed with various CR models which are implemented in the PYTHIA 6.1 Monte Carlo program [11].

The models SKI and SKII [2] are based on the analogy between coloured strings and superconductors of type I or II with either a finite transverse size or with no lateral extent. The reconnection occurs at the crossing of the two string entities (elongated bags or vortex lines).

The GH model is an implementation in PYTHIA of the model described in Reference 3 where the reconnection is allowed only if it reduces the string length. The reconnection probability in this implementation is 92% as compared to 34% and 32% in the SKI and SII models respectively.

Colour reconnection effects could appear as a depletion or an enhancement of particle production between the quark jets. Figure 11 (left) shows the particle flow distributions obtained with the PYTHIA Monte Carlo at particle level for particles having a momentum greater than 100 MeV. The full line corresponds to no colour reconnection while the dashed line corresponds to the prediction from the GH model implemented in PYTHIA. The interjet regions corresponding to the two W bosons are named A and B while the interjet regions between two jets from different W's are named C and D as indicated on the plot. We observe that the GH model gives some depletion in the regions A and B and some enhancement of particle rates in the regions C and D, as expected.

For flow distributions computed as a function of the rescaled angle, regions A and B, as well as regions C and D, can be averaged in order to reduce the statistical uncertainty. The averaged results are shown in the two bottom plots of Figure 11. Figure 12 shows the same distributions obtained at detector level using all clusters. The effects seen at the detector level are consistent with the particle level results and have similar amplitudes.

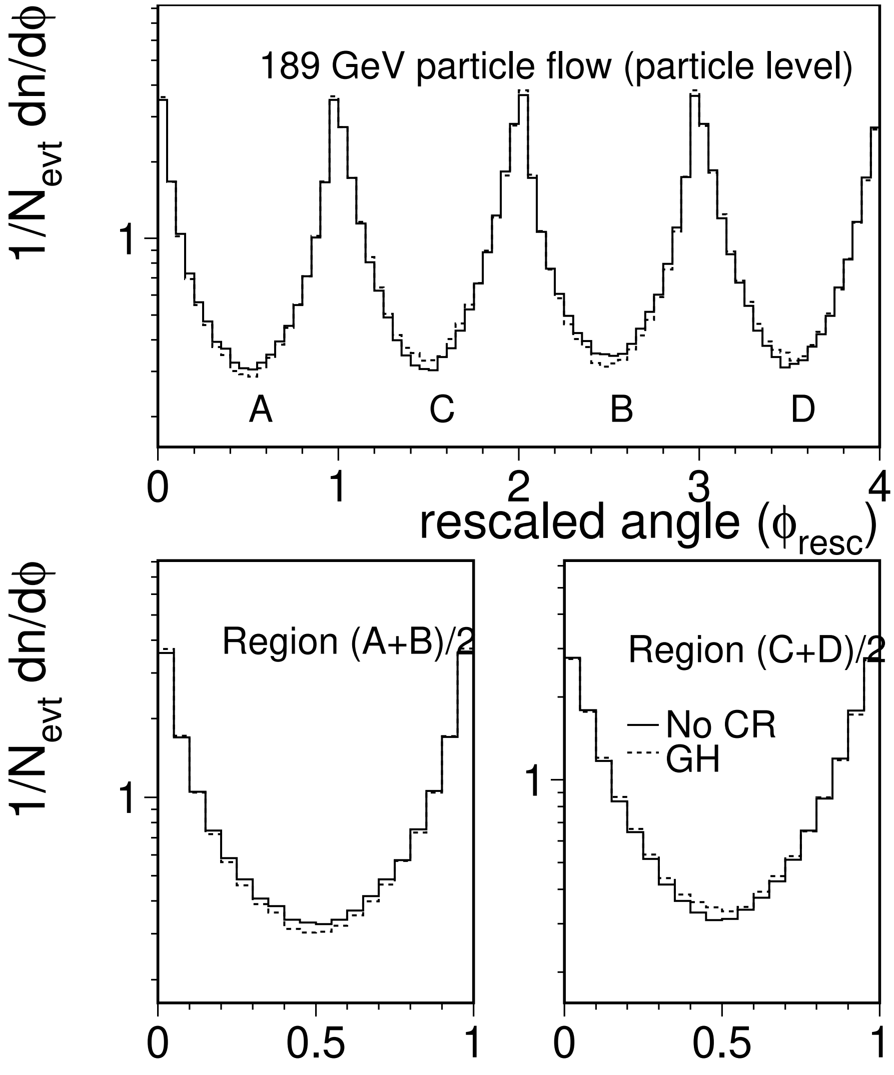

Figure 11: PYTHIA prediction at $\sqrt{s} = 189$ GeV for the particle flow distribution at particle level without colour reconnection (No CR) and for the GH model.

The ratio of the particle activity between the quarks from the same W (regions A+B) and the particle activity between quarks from a different W (regions C+D) is found to be a sensitive observable to the cross-talk effects. This ratio computed from the particle flow distributions at particle level and at detector level as a function of the rescaled angle ϕ_{resc} is shown in Figure 13 (left and right). The full line corresponds to the PYTHIA prediction without CR, the dashed line is the prediction from the SK I scenario, and the dotted line corresponds to the prediction of the GH model. The dots are the L3 data for the detector level distribution.

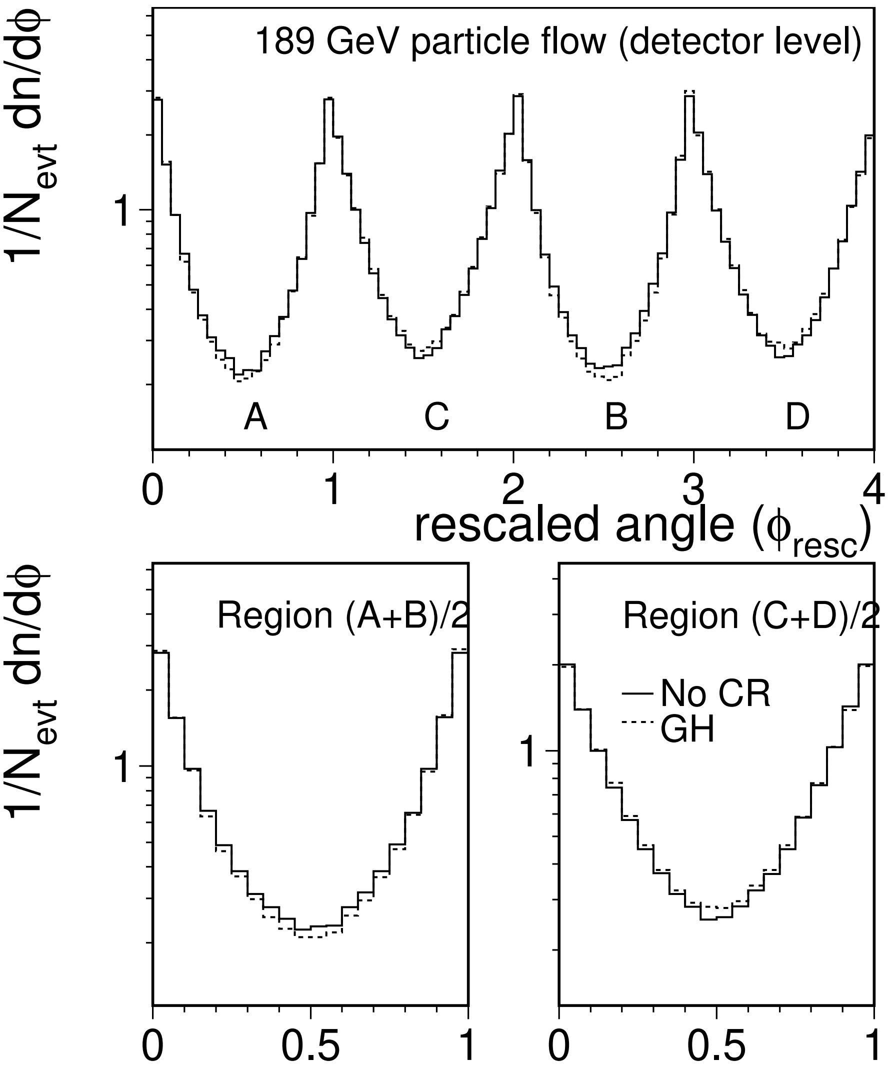

Figure 12: PYTHIA prediction at $\sqrt{s} = 189$ GeV for particle flow distribution at detector level without colour reconnection (No CR) and for the GH model.

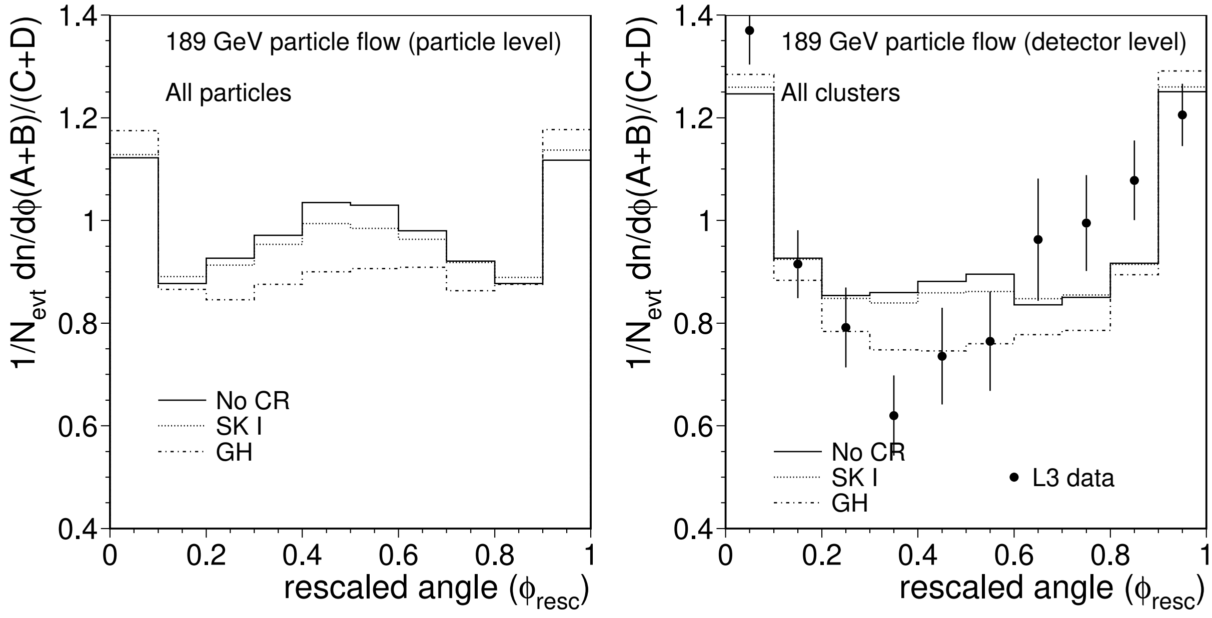

Figure 13: Ratio (R) of the particle flow in regions (A+B) divided by the particle flow in regions (C+D) at particle level on the left and at detector level on the right.

The differences between the models with and without reconnection schemes are larger in the middle of the interjet regions. Therefore, in order to quantify the colour reconnection effects the ratio R is computed in a restricted $\phi_{\rm resc}$ interval ranging from 0.3 to 0.7. The corresponding variables for particle and energy flow are defined as follows:

$$R_N = \frac{\int_{0.3}^{0.7} \frac{1}{N} \cdot \frac{dn}{d\phi}(regionsA{+}B)}{\int_{0.3}^{0.7} \frac{1}{N} \cdot \frac{dn}{d\phi}(regionsC{+}D)} \quad \text{and} \quad R_E = \frac{\int_{0.3}^{0.7} \frac{1}{E} \cdot \frac{dE}{d\phi}(regionsA{+}B)}{\int_{0.3}^{0.7} \frac{1}{E} \cdot \frac{dE}{d\phi}(regionsC{+}D)}$$

The values obtained for R_N and R_E using all particles at particle level and all clusters at detector level are given in Tables 4 and 5 for the model without CR and for the SKII, SKI and GH models.

The SK models show effects of the order of a few % with these variables while the GH model implemented in PYTHIA (having a high reconnection probability) shows a larger effect of about 10%. The magnitude of these effects are not changed between particle and detector levels.

The dependence on the reconnection probability has been investigated with the SKI model. We have used the “Crete” sample (see section 2) with 100% of the events colour-reconnected, and mixed it with MC samples without colour reconnection. The events are generated with ALEPH tuning parameters and do not contain any Bose-Einstein correlations; they have been fully simulated in the L3 detector.

The ratios R_E and R_N have been computed at particle and detector levels for several reconnection probabilities. The results are shown in Figure 14. It appears clearly that even if the absolute value changes between particle and detector level, due to particle resolution effects and overlapping clusters, the relative dependence on the reconnection probability is not degraded by detector effects. From the slope of the dependence we can also see that R_N gives more sensitivity to colour reconnection than R_E knowing that the statistical error should be of the same order for the 2 ratios.

Model	R_N particle	R_N detector
No CR	0.999 ± 0.007	0.868 ± 0.007
SkII	0.985 ± 0.007	0.855 ± 0.007
SKI	0.986 ± 0.007	0.852 ± 0.007
GH	0.898 ± 0.006	0.758 ± 0.006

Table 4: Values of R_N at particle and detector level

Model	R_E particle	R_E detector
No CR	0.812 ± 0.009	0.696 ± 0.009
SkII	0.790 ± 0.009	0.680 ± 0.009
SKI	0.791 ± 0.009	0.675 ± 0.009
GH	0.710 ± 0.008	0.615 ± 0.008

Table 5: Values of R_E at particle and detector level

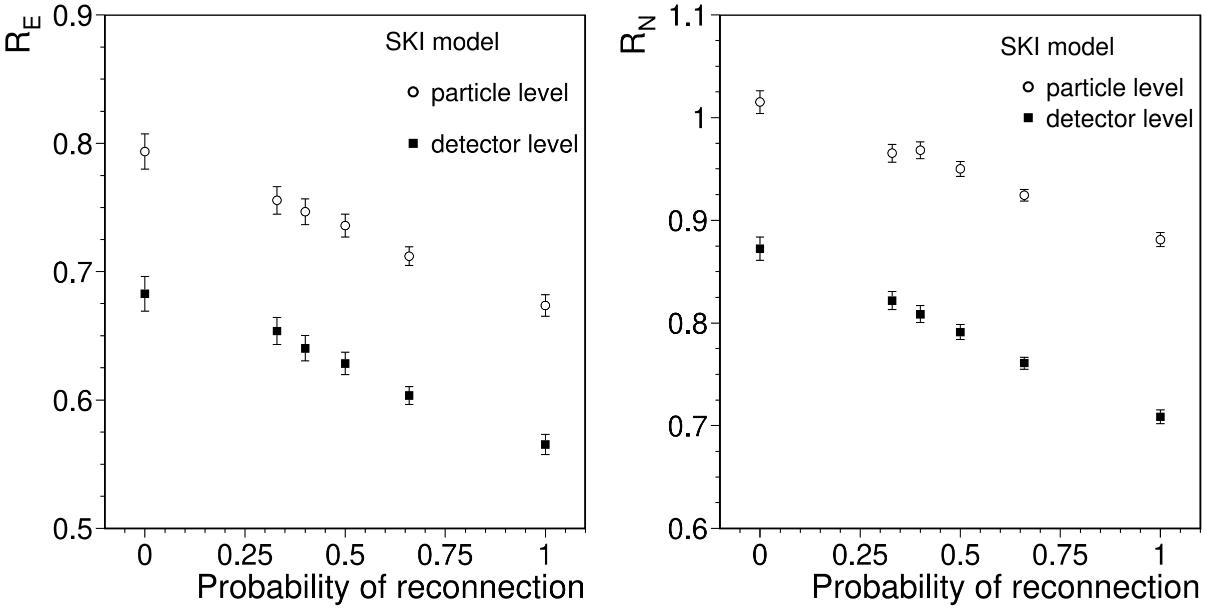

Figure 14: The ratios R_E and R_N at particle level and detector level as a function of the reconnection probability for the SKI model.

The ratio values obtained with the data using all clusters are:

$$R_N = 0.771 \pm 0.049(stat.) \quad (6)$$
$$R_E = 0.593 \pm 0.058(stat.)\,, \quad (7)$$

where the error quoted is only statistical.

3.4 Systematic uncertainties

Several sources of systematic errors have been investigated.

- Possible effects coming from Bose-Einstein correlations in hadronic W decays have been estimated by repeating the measurements with several Monte Carlo options: BE_0, BE_{32} and No BE. The results are summarised in Figure 15. The sensitivity of these variables to Bose-Einstein correlations seems small and the corresponding error is given by the spread in the measured values for the considered options.

- Systematic effect from quark fragmentation modelling has been estimated by comparing results using JETSET and HERWIG Monte Carlo programs. The error is obtained by taking half of the difference between the two models. The values are shown in Figure 15. They were obtained from Crete files generated with the ALEPH parameters. It should be noted that the JETSET results obtained with the L3 parameters (called PYTHIA BE_{32} in the figure) are fully consistent with the JETSET results obtained with the different fragmentation parameters used to generate the Crete samples.

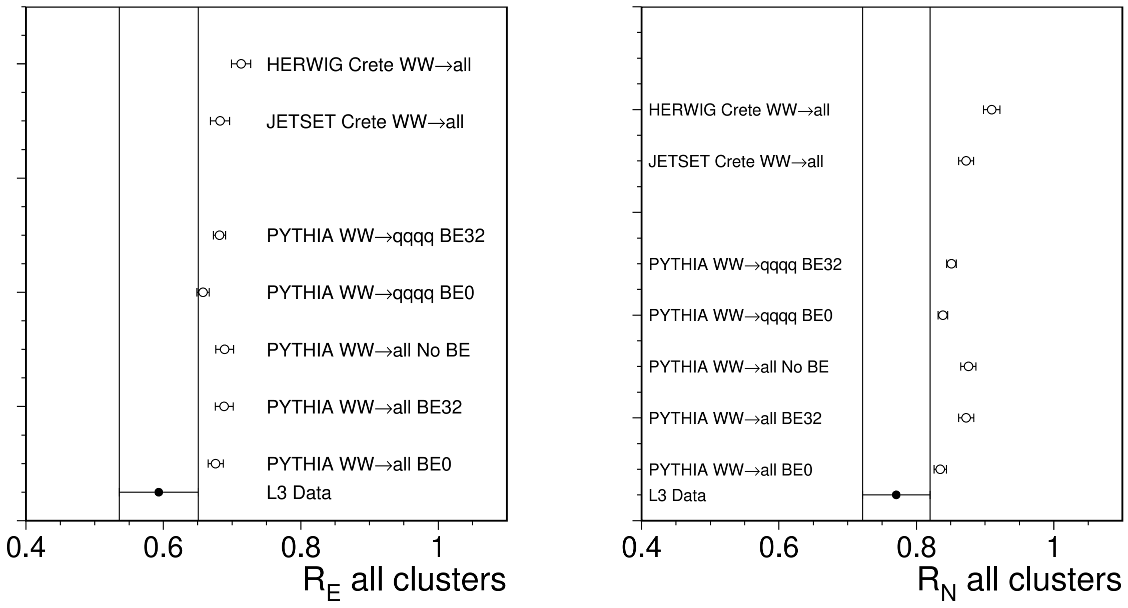

Figure 15: The ratios R_E and R_N at detector level for several Monte Carlo models without Colour Reconnection. The black dot and the band represents the data values with the statistical error only.

source	R_E	R_N
BEC	$\pm$ 0.011	$\pm$ 0.017
Fragmentation	$\pm$ 0.015	$\pm$ 0.018
back.	$\pm$ 0.005	$\pm$ 0.007
Flow objects	$\pm$ 0.007	$\pm$ 0.014
Total	$\pm$ 0.020	$\pm$ 0.029

Table 6: Contributions to the systematic uncertainties on R_E and R_N.

- Since the $q\bar{q}$ background which is subtracted corresponds mainly to QCD 4-jet events which are not well modelled by parton shower programs (their rate is too low in MC), the systematic uncertainty coming from this source has been estimated by varying the corresponding cross-section by $\pm10\%$. The resulting error is the smallest contribution to the total systematic uncertainty.
- An other important systematic test is to verify the dependence of the result with the definition of energy flow objects. This is done by comparing results obtained only from calorimetric clusters and results obtained by objects built from combination of track and calorimetric clusters, the latter being the nominal choice. Since these 2 different energy flow objects have different energy resolution acceptance and overlap probability the absolute values of the ratios cannot be directly compared. Instead the ratio between the 2 different results have been obtained for 12 different MC samples having different fragmentation options and different colour reconnection schemes. The spread of the 12 values gives an estimate of the stability of the results with the choice of the flow objects. It is observed that R_N is more sensitive to this choice than R_E as we may expect from their definitions.

A summary of the different contributions to the systematic errors is given in Table 6.

The ratio values obtained with the data using all clusters are then:

$$R_N = 0.771 \pm 0.049(stat.) \pm 0.029(syst.) \tag{8}$$
$$R_E = 0.593 \pm 0.058(stat.) \pm 0.020(syst.)\,, \tag{9}$$

3.5 Comparison with models

Figure 16 shows a comparison of R_E and R_N at detector level with several Monte Carlo models including colour reconnection. The dot with error shows the data value with the statistical error only while the band width corresponds to the total error taken as the sum in quadrature of the statistical and systematic components.

From the numbers given previously we see that the data deviates from the PYTHIA No CR scenario by about 1.7 standard deviations and that the data prefer models having some colour reconnections.

Figure 17 shows the compatibility of the results with the predictions from SKI model. The shaded bands in the bottom part show the SKI predictions as a function of the reconnection probability for R_E (left) and R_N (right). The point is the L3 measurement with horizontal band showing the 1 sigma boundary.

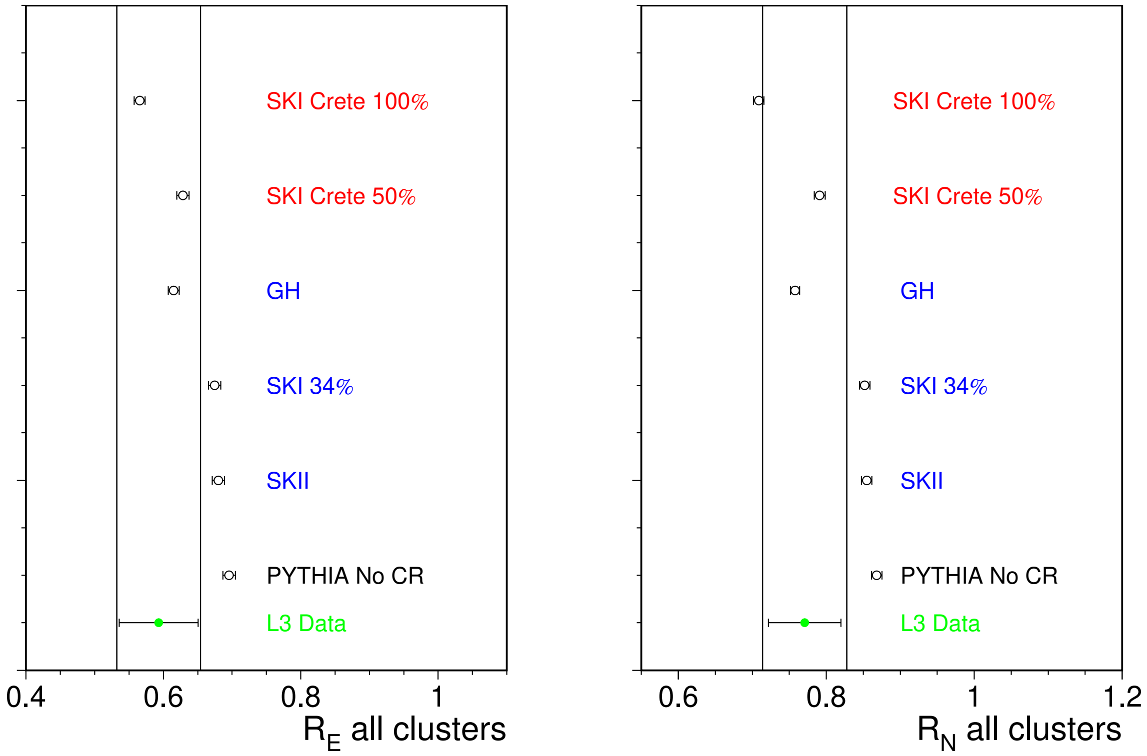

Figure 16: The ratio R_E and R_N at detector level for several Monte Carlo models with and without Colour Reconnection. The black dot with the error bar shows the data with the statistical error only while the band corresponds to the sum in quadrature of the statistical and systematic error components.

The comparison has also been done with the shape of the interjet flow distributions over the whole angular range. The χ^2 of the data distributions have been computed with respect to the SKI distributions over all 10 bins of the rescaled angle ranging from 0 to 1.

The resulting χ^2 values are shown in the top part of Figure 17 as a function of the reconnection probability. The χ^2 shows a minimum for a reconnection probability of $\approx$40% with the SKI model.

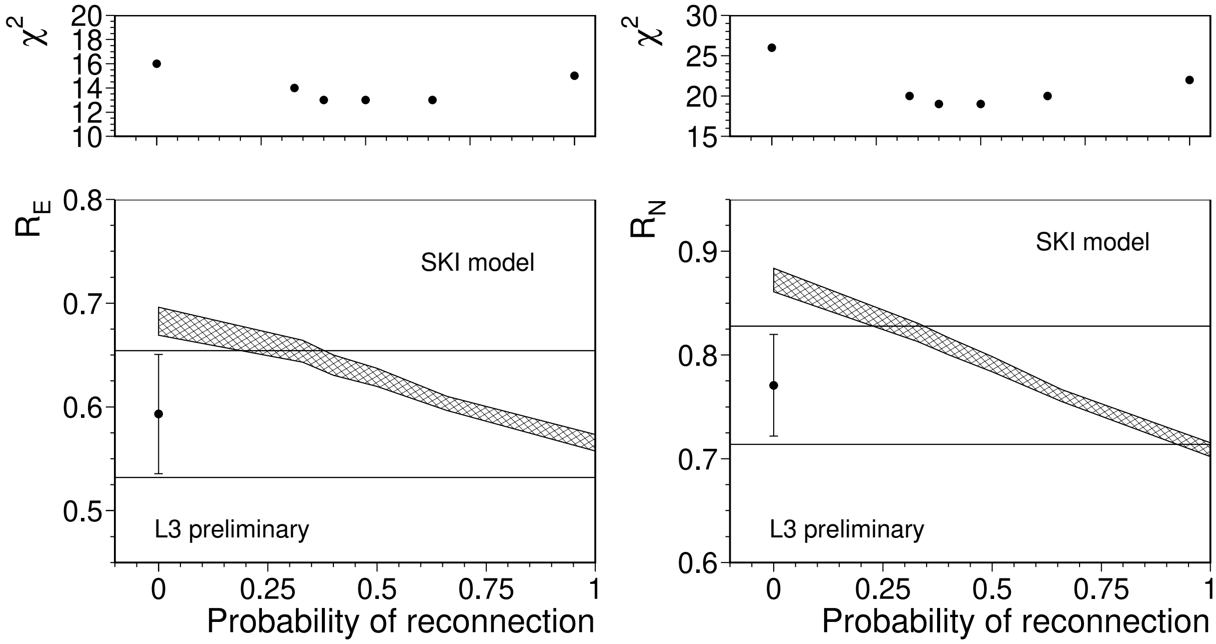

Figure 17: The ratio R_E and R_N at detector level as a function of the reconnection probability for the SKI model. The top part shows the χ^2 value obtained by comparing the whole angular range data distributions with SKI predictions, in 10 bins.

3.6 Asymmetry variables

The other set of variables, corresponding to asymmetries in particle- and energy population between jets, and reported as being more sensitive to differences between CR models [5] are still under investigation. For the time being there is no update of what has been given in Reference 6.

4 Conclusions

Within the statistics of the 183-202 GeV data samples, no significant differences between charged particle production in the hadronic final state of $qqqq$ and $qq\ell\nu$ events are observed. This holds for the average charged particle multiplicity as well as for the multiplicity distribution as a function of particle momentum. The difference in charged multiplicity is also compatible with the predictions of the PYTHIA SK I and SK II models. These results are preliminary; they are in agreement with our earlier results [6, 13], as well as similar studies performed by the other LEP experiments [14].

Despite the fact that the statistical error on the data is still too large to have a definite answer on the existence or not of colour reconnection effects in hadronic decays of W pairs, the method used in this analysis appears promising. The preliminary results obtained with the L3 data at 189 GeV show a 1.7 sigma deviation with the PYTHIA model without colour reconnection effects. In the framework of the SKI model and assuming that the effect can be reproduced by this model the data tends to favour a 40% reconnection probability.

The analysis presented in this note is an analysis in progress. The selection may to be reoptimised to try to improve the efficiency. This selection is mainly based on the W boost and should be reestimated at each different e^+e^- centre-of-mass energy given by LEP.

An important cross-check of the method is the comparison of results obtained with actual 4-jet hadronic W^+W^- decays to results from 4-jet events obtained by mixing semi-leptonic events (free of any cross-talk effects), as performed for example in Reference 15; also this comparison is in progress.

A good understanding of the systematics together with an increase of the statistics and some optimisation of the selection should lead to sufficient discrimination power among the various CR models to see whether the data agree or not with the standard Monte Carlo without colour reconnections.

References

[1] G. Gustafson, U. Pettersson and P. Zerwas, Phys. Lett. **B 209** (1988) 90.

[2] T. Sjöstrand and V. Khoze, Z. Phys. **C 62** (1994) 281; V. Khoze and T. Sjöstrand, Eur. Phys. J. **C 6** (1999) 271.

[3] G. Gustafson and J. Häkkinen, Z. Phys. **C 64** (1994) 659.

[4] Proceedings of the workshop "Physics at LEP 2", CERN Yellow Report 96-01.

[5] D. Duchesneau, "*New method based on energy- and particle-flow in* $e^+e^- \to W^+W^- \to$*hadrons events for colour reconnection studies*", preprint LAPP-EXP 2000-02. http://wwwlapp.in2p3.fr/preplapp/psexp/lappexp0002.ps.gz.

[6] The L3 Collaboration, *Search for Colour Reconnection Effects in* $e^+e^- \to W^+W^- \to$ *hadrons through multiplicity and Energy- and Particle-Flow Studies*, L3 Note 2503 (2000), submitted to the 2000 Winter Conferences.

[7] L3 Collab, B. Adeva et al., Nucl. Instr. and Meth. **A 289** (1990) 35;
M. Chemarin et al., Nucl. Instr. and Meth. **A 349** (1994) 345;
M. Acciarri et al., Nucl. Instr. and Meth. **A 351** (1994) 300;
G. Basti et al., Nucl. Instr. and Meth. **A 374** (1996) 293;
I. C. Brock et al., Nucl. Instr. and Meth. **A 381** (1996) 236;
A. Adam et al., Nucl. Instr. and Meth. **A 383** (1996) 342.

[8] S. Jadach and K. Zalewski, Acta. Phys. Pol. **B 28** (1997) 1363;
V. Kartvelishvili, R. Kvatadze and R. Møller, Phys. Lett. **B 408** (1997) 331;
K. Fialkowski and R. Wit, Z. Phys. **C 74** (1997) 145;
K. Fialkowski, R. Wit and J. Wosiek, Phys. Rev. **D 58** (1998) 094013.

[9] The L3 Collaboration, *Preliminary Results on the Measurement of W-Pair Production in e^+e^- Interactions at $\sqrt{s} = 189$ GeV and W-decay Branching Fractions*, L3 Note 2376 (1999), paper #6_253 submitted to the International Europhysics Conference High Energy Physics 99, Tampere, Finland, 15-21 July 1999.

[10] The L3 Collaboration, *Preliminary Results on the Measurement of W-Pair Production in e^+e^- Interactions at $\sqrt{s} = 192 - 202$ GeV and W-decay Branching Fractions*, L3 Note 2514 (2000), submitted to the 2000 Winter Conferences.

[11] Pythia Monte Carlo Program:
T. Sjöstrand, CERN-TH-7112/93 (1993), revised august 1995;
T. Sjöstrand, Comp. Phys. Comm. **82** (1994) 74.

[12] S. Jadach, B. F. L. Ward and Z. Wąs, Phys. Lett. **B 449** (1999) 97.

[13] The L3 Collaboration, M. Acciarri et al., L3 Note 2278 (1998), paper #507 submitted to the International Conference on High Energy Physics 1998, Vancouver, Canada, 1998.

[14] DELPHI Collab, P. Abreu et al., Phys. Lett. **B 416** (1998) 233, DELPHI Note 98-16 CONF 117 (1998), DELPHI Note 99-21 MORIO CONF 220 (1999);
OPAL Collab, K. Ackerstaff et al., Eur. Phys. J. **C 1** (1998) 395, G. Abbiendi et al., Phys. Lett. **B 453** (1999) 153, OPAL Physics Note PN 412 (1999);
ALEPH Collab, R. Barate et al., ALEPH Note 98-066 CONF 98-036 (1998), ALEPH Note 99-026 CONF 99-020 (1999).

[15] The L3 Collaboration, M. Acciarri et al., *Bose-Einstein Correlations in $e^+e^- \to W^+W^-$ Events at $\sqrt{s} = 189$ GeV*, L3 Note 2499 (2000), paper submitted to the Winter Conferences 2000.